

Identifying and Assessing Debris Strikes in NASA Spacecraft Telemetry

Anne Aryadne Bennett^{1,2} and Hanspeter Schaub³

¹University of Colorado Boulder, 3775 Discovery Dr, Boulder, CO 80303. anne.a.bennett@colorado.edu

²Northrop Grumman Innovation Systems, 45101 Warp Dr, Dulles, VA, 20166.

³University of Colorado Boulder, 3775 Discovery Dr, Boulder, CO 80303. hanspeter.schaub@colorado.edu

ABSTRACT

Debris strikes on operational spacecraft are becoming more common due to increasing numbers of space objects. Sample return missions indicate hundreds of minor strikes, but rigorous analysis is often only performed when a strike causes an anomaly in spacecraft performance. Developing techniques to identify and assess minor strikes that do not immediately cause anomalous behavior can help to validate models for debris populations, perform risk assessments, and aid in the attribution of future anomalies. This study applies change detection algorithms to telemetry from three NASA missions to identify potential debris strikes. The primary method for detection is applying a sequential probability ratio test to the spacecraft's angular momentum to detect subtle, unexpected, abrupt changes. Each spacecraft's telemetry has unique characteristics which interfere with strike detection so methods are developed to clean the telemetry for accurate detection. A selection of potential debris strikes identified with these algorithms are cross-checked against other telemetry to ascertain the plausibility of a debris strike. Detected strikes are cataloged and the results are discussed in the context of expected strike sources and potential causes of false alarms. Developing the capability to catalog and characterize minor debris strikes using normal telemetry allows any active spacecraft to be used as an *in situ* debris sensor.

1 INTRODUCTION

The population of trackable fragmentation debris has more than doubled in the past 25 years [1]. This is especially concerning because while trackable debris can be avoided by maneuvering satellites, most fragmentation events also release clouds of debris too small to track. The Space Surveillance Network (SSN) tracks debris down to around 10 cm in LEO and 70 cm in GEO, but a <1 cm piece of debris can cause catastrophic damage to a spacecraft if it hits a sensitive component, as shown in Figure 1(a). As of January 2019 there are approximately 34,000 debris objects greater than 10 cm in orbit, but there are approximately 900,000 objects between 1 cm and 10 cm. Therefore, well under 10% of the potentially hazardous debris population is tracked.

The situation is especially dire in GEO where many valuable spacecraft are located. Since GEO is unreachable by ground-based radar measurements and there are no sample return missions the small debris environment is largely unknown. NASA's orbital debris model, ORDEM3.0, only models debris down to 10 cm in GEO leaving a significant population of potentially harmful debris that is entirely uncharacterized. Even that 10 cm boundary is an extension from debris measurements; the GEO debris models are based on measurements taken by the MODEST telescope which measured pieces 30 cm and larger. This might account for abrupt anomalies that several GEO spacecraft have experienced in recent years. For example, in April 2019 Intelsat-29e experienced an abrupt anomaly resulting in a fuel leak and shed debris, culminating in the total loss of the satellite. The failure review board concluded that the anomaly was caused by either a particle strike or an electrostatic discharge event coupled with an existing harness flaw [2]. In other events, such as the Telkom-1 mishap, ground-based telescopes have recorded satellites spontaneously spewing clouds of debris and contributing to the untrackable debris population.

However, not all debris strikes are fatal. In August of 2016 the Sentinel-1A spacecraft experienced an anomaly consisting of an abrupt attitude perturbation (Fig. 1(b)) coupled with a slight orbit change and simultaneous decrease in solar power output. On-board cameras confirmed a debris strike on the solar array. However, the solar array strike was non-catastrophic and operations continued nominally [3]. Similar events have been detected on NASA's MMS spacecraft, where anomalous behaviors have been noticed and attributed to debris strikes, but the effects were

recoverable and operations continued nominally [4]. In addition to these large and obvious strikes, small strikes occur on spacecraft without even perturbing operations. Sample return missions such as the Long Duration Exposure Facility and the Hubble solar arrays have cataloged hundreds to thousands of minor debris craters after a few years on orbit (Figure 1(c)) [5].

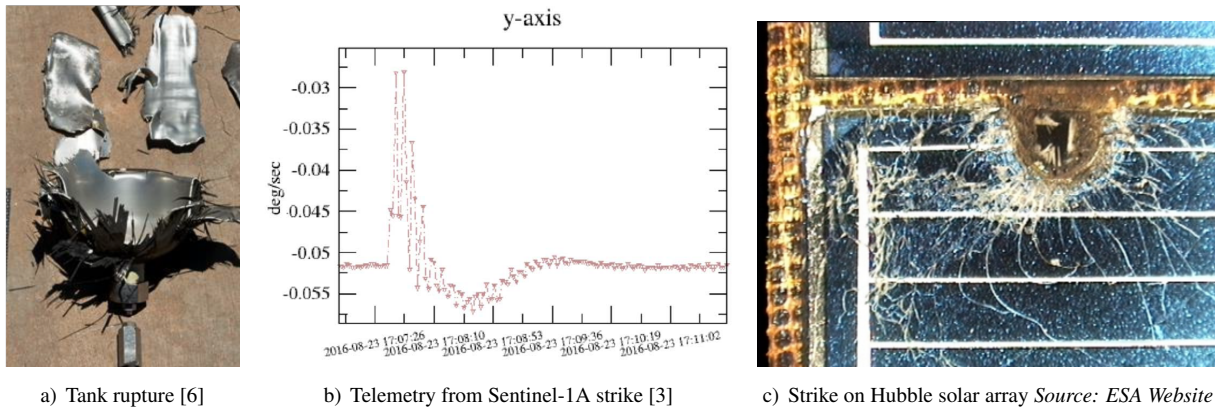


Figure 1: Examples of small debris impact effects. The tank in a) was impacted by a 2 mm aluminum sphere. The hole in c) is 2.5 mm

Other constellations have experienced events like Sentinel-1A, and a recent report by the NASA Engineering and Safety Center (NESC) incorporated these events into a study comparing observed anomalies to failures predicted using current debris models (ORDEM3.0). The NESC report assessed reported vs. predicted failures for several LEO satellite systems. For one LEO constellation seven events had been observed where satellites experienced sudden unexpected movements thought to be caused by debris. These movements consisted of abrupt changes in satellite mean altitude and/or rotation rates. Comparing these and other events to predicted events, the NESC report found very low correlation between the on-orbit events and the ORDEM3.0 predictions. ORDEM3.0 predicts a substantially higher risk of failures than these LEO systems have experienced [7]. This indicates that current LEO debris models are overly conservative, which is burdensome for ongoing programs as it makes it difficult to show compliance with debris mitigation standards. One of the recommendations of the NESC report is to collect data on satellite orbital perturbations and momentum changes. This paper applies that recommendation by examining telemetry of several NASA spacecraft and applying change detection (CD) algorithms to highlight potential debris impacts, even when they don't cause anomalous behavior. It is important to understand these debris populations even if many strikes are benign, since a similarly-sized piece of debris impacting a critical component can result in catastrophic failure.

The NASA missions evaluated consist of the Solar Dynamics Observatory (SDO) in GEO, the Magnetospheric Multiscale (MMS) constellation in a highly elliptical orbit, and the Fermi spacecraft in LEO. This research is ongoing and this paper represents the current status, including methods and some early results. Section 2 discusses the methods that are applied in this paper. The cumulative sum sequential probability ratio test (CUSUM SPRT) is applied to the angular momentum per reference [8]. Section 3 discusses the telemetry pre-processing necessary to prepare data for the CD algorithm. Each mission has a unique instrument suite and telemetry output, so custom algorithms are developed for each mission. An abrupt change in the angular momentum is indicative of a strike and causes a spike in CUSUM SPRT filter output. However, mission events also trip the debris strike detection algorithms so additional filters are developed to clean the telemetry by blanking results during mission events or pre-processing the data to remove known features. The preliminary results are provided in Section 4, and include both summarized data and telemetry showing specific events.

2 ANALYSIS METHODS

The angular momentum of a spacecraft, when expressed in an inertial frame, is quiescent in the absence of external forces. Per reference [8], this allows the application of canonical change detection techniques to detect abrupt changes in the angular momentum of the spacecraft. A micrometeoroid or orbit debris (MMOD) impact applies an external force and creates an abrupt change in a satellites' angular momentum. In this paper, these abrupt changes are detected using a CUSUM SPRT. This test is selected because it produces a high signal-to-noise ratio and predictable

false alarm rate on simulated data. A robust and accurate algorithm is required on real-world telemetry, since the noise is less predictable than simulated data and unexpected features manifest as debris strikes.

A sliding window filter is used to apply the CUSUM SPRT to the momentum telemetry. The CUSUM SPRT utilizes a likelihood ratio test, \mathcal{L} , which is based on the probability density functions of the null and alternative hypothesis. It compares the likelihood of seeing each datapoint under an alternative hypothesis (debris strike) to the likelihood under the null hypothesis (no debris strike).

$$\mathcal{L}(\mathbf{y}) = \frac{p(\mathbf{y}|\mathcal{H}_1)}{p(\mathbf{y}|\mathcal{H}_0)} \quad (1)$$

Where $p(\mathbf{y}|\mathcal{H}_i)$ is the probability of \mathbf{y} given hypothesis \mathcal{H}_i . The CUSUM algorithm sums the log of the likelihood ratio test sequentially to give the test statistic S_n .

$$S_n = \sum_{k=1}^n \ln(\mathcal{L}(\mathbf{y})) \quad (2)$$

The parameter S_n trends negative when the samples, as a whole, are more likely to be from \mathcal{H}_0 than \mathcal{H}_1 , and trends positive when they are more likely from \mathcal{H}_1 . This change in drift is detected through

$$W_n = S_n - \min_{0 \leq k < n} S_k \quad (3)$$

The filter output, W_n , stays close to zero while S_n trends downward, then grows if it trends upward.

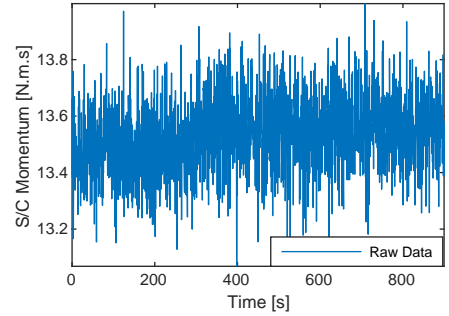
The algorithm is applied in a sliding window, which is prepended with a pre-window that is used to derive the expected distribution parameters. The samples in the post-window are compared to the distribution observed in the pre-window, so when an abrupt change occurs at the junction between the windows the output of the filter displays a spike even if that change is small relative to the typical variation in the data. Figure 2 illustrates a distribution change and the resultant filter output using simulated data. Figure 2(a), shows the raw momentum telemetry, 2(b) shows the distribution parameters overlaid on the telemetry to highlight the change, and 2(c) shows the filter output when run against that telemetry.

3 PRE-PROCESSING TELEMETRY

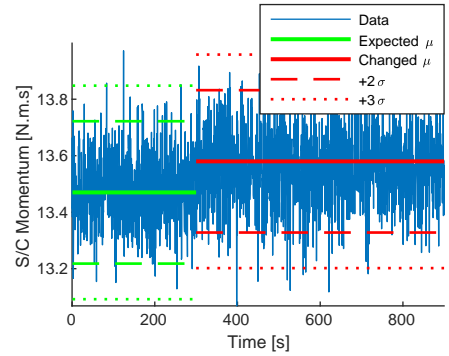
Each NASA mission examined has a unique design incorporating different hardware suites and therefore unique telemetry. Each spacecraft also has mission events and telemetry features which trip the debris strike detection thresholds and must therefore be blanked from the overall results. The following sections describe the methods applied to each spacecraft obtain quiescent angular momentum telemetry and clean it so that CUSUM SPRTs can be applied effectively.

3.1 Solar Dynamics Observatory

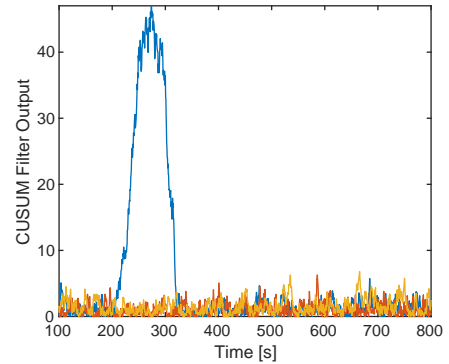
The Solar Dynamics Observatory (SDO) is a three-axis stabilized spacecraft in GEO orbit which stares at the sun. Since its body frame is aligned with the sun vector it rotates very slowly with respect to inertial, so the body-frame momentum, as calculated on-board, is used to apply the impact detection algorithms.



a) Raw simulated telemetry



b) With distribution changes



c) Filter output

Figure 2: Simulated momentum telemetry showing debris strike at $t=300s$, with distribution changes highlighted and associated filter output showing peak at time of strike

SDO’s angular momentum telemetry exhibits a square wave with a period of approximately 13 minutes. This square wave is fairly consistent across years of data, but each occurrence manifests as an abrupt change in angular momentum of exactly the type that these filters are designed to detect. This feature is removed from the data by designing a notch filter that eliminates the frequencies for both the square wave and a low-frequency (2 per day) oscillation that the data displays. The edges of this filter show some effects that manifest as debris strikes, so the filter is run on 10 days of data at a time and the junction between the data sets is blanked.

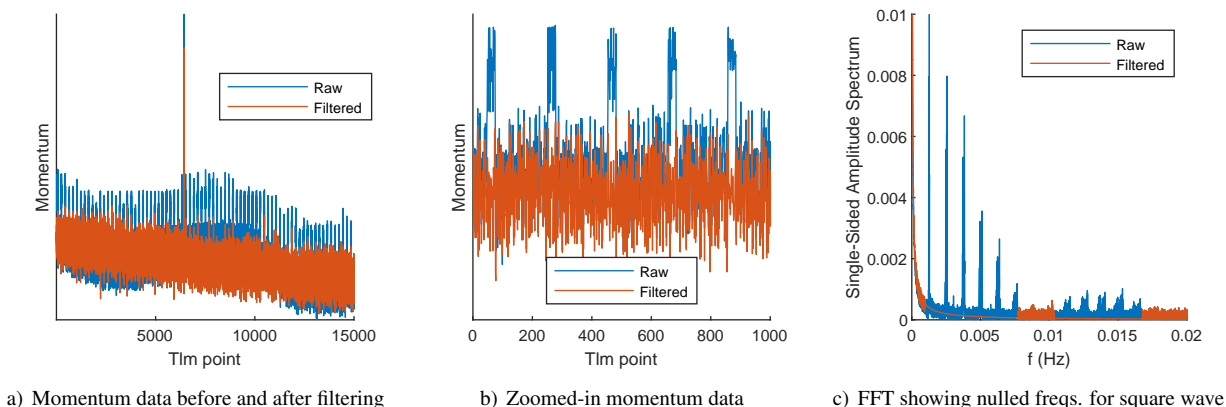


Figure 3: Filtering SDO angular momentum telemetry to remove periodic signatures

SDO’s strike detection filters trip whenever the thrusters fire for a station-keeping or momentum-dumping maneuver, so all thruster firings are blanked from the data. Since the body-frame momentum is used slewing maneuvers also trip the threshold and are blanked, but these occur infrequently. The spacecraft performs reaction wheel reconfigurations to avoid zero crossings, but the filters are robust to these and they do not need to be blanked.

To set the detection threshold a day of data is plotted and obvious spikes are removed to show the no-strike noise floor. A kernel distribution is fitted to each axis and the resulting probability density function is used to develop the threshold. The thresholds are set such that the probability of exceeding the threshold equates to one in the number of telemetry points downlinked each day, for an approximate false alarm rate of one per day. This produces a similar threshold in each axis since the noise levels are similar, so an average value is selected as the threshold for all three axes.

3.2 MMS Mission

The MMS mission consists of four spacecraft flying in formation in a highly elliptical orbit. These spacecraft are spin-stabilized and have long wire booms and other appendages. They have thrusters for constellation resizing and other maneuvers, but they do not have reaction wheels. Startrackers provide quaternions and rates are derived from attitude data. With this telemetry the inertial angular momentum (${}^N\mathbf{H}$) of each MMS spacecraft is calculated via ${}^N\mathbf{H} = [NB][I_{sc}]{}^B\boldsymbol{\omega}$, where $[NB]$ is the direction cosine matrix to convert from the body frame to the inertial frame, $[I_{sc}]$ is the inertia of the spacecraft, and ${}^B\boldsymbol{\omega}$ is the angular rate of the spacecraft expressed in body-frame coordinates.

The MMS spacecraft’s appendages cause unique behaviors that manifest as MMOD strike detections. Whenever the spacecraft goes through perigee the inertial angular momentum experiences a change, as shown in Figure 4(a). Whenever the thrusters fire these appendages begin to oscillate, and it takes several days for those oscillations to damp out such that the observed rigid-body momentum calculation no longer trips the debris strike detection thresholds. Figure 4 illustrates both of these effects. To mitigate them, the telemetry is blanked during perigee passages, and for 10 days after each thruster firing.

The detection thresholds for MMS are set in a manner similar to those for SDO. However, MMS data doesn’t often exhibit the distinct spikes seen in SDO telemetry so only the perigee effects are removed. Also, each axis exhibits a different noise level so the thresholds are set independently for each axis rather than being averaged.

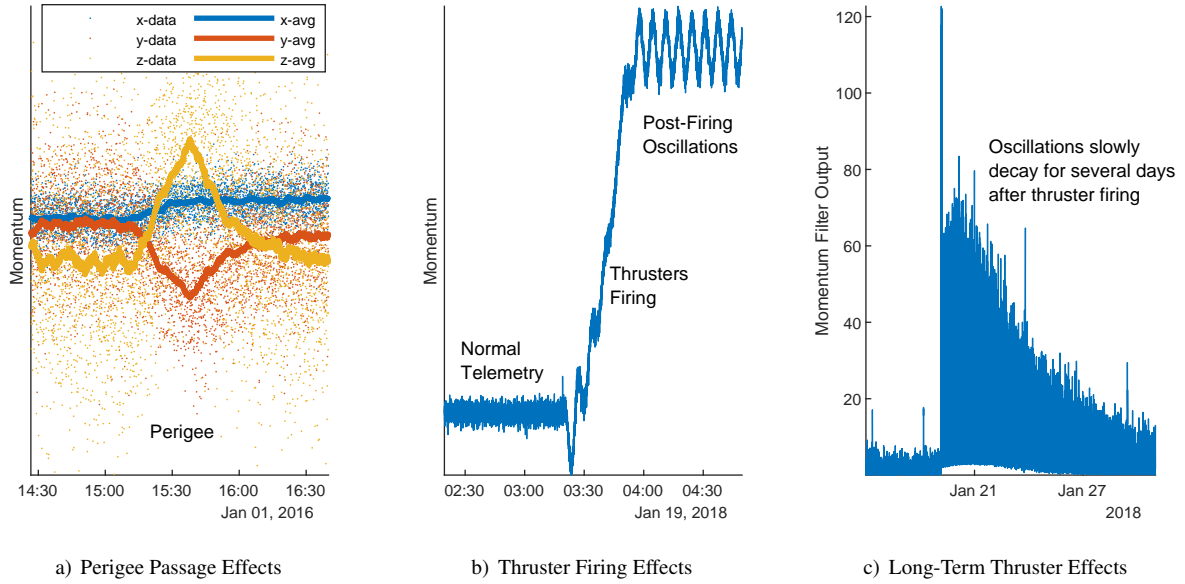


Figure 4: Effects of mission events on MMS inertial angular momentum

3.3 Fermi

The Fermi spacecraft is a very agile spacecraft in LEO. It is three-axis controlled using reaction wheels and slews constantly to observe various parts of the sky. It uses magnetic torquer bars to control its angular momentum which presents a unique challenge as the angular momentum is changing constantly. Therefore a proxy momentum, \mathbf{H}^* , is calculated to negate the effects of the torquer bars and produce a relatively quiescent momentum for debris strike analysis. First, the inertial angular momentum, ${}^{\mathcal{N}}\mathbf{H}$ and change in momentum due to the torquer bars, ${}^{\mathcal{N}}\dot{\mathbf{H}}$, are calculated as follows

$${}^{\mathcal{N}}\mathbf{H} = [NB][I_{sc}]^{\mathcal{B}}\boldsymbol{\omega} + [NB] \sum_{i=1}^N [BW]_i \begin{bmatrix} I_{ws}\Omega_i \\ 0 \\ 0 \end{bmatrix} \quad (4)$$

$${}^{\mathcal{N}}\dot{\mathbf{H}} = [NB]^{\mathcal{B}}\mathbf{L} = [NB](d_{mt} \begin{bmatrix} I_x \\ I_y \\ I_z \end{bmatrix} \times {}^{\mathcal{B}}\mathbf{B}) \quad (5)$$

where ${}^{\mathcal{B}}\mathbf{L}$ is the torque applied to the spacecraft in body frame coordinates, d_{mt} is the magnetic dipole of the torque rods, I_x , I_y , and I_z are the current applied to each torque rod (which are aligned with the body frame axes), and ${}^{\mathcal{B}}\mathbf{B}$ is the magnetic field as measured by on-board sensors in body frame coordinates. Then, \mathbf{H}^* is calculated by applying a sliding window to the data and propagating each ${}^{\mathcal{N}}\mathbf{H}$ forward in time using ${}^{\mathcal{N}}\dot{\mathbf{H}}$. It is propagated for the length of the CUSUM algorithm's sliding window, and then the difference between the propagated ${}^{\mathcal{N}}\mathbf{H}$ and the true ${}^{\mathcal{N}}\mathbf{H}$ is used as \mathbf{H}^* . In theory, given accurate propagation the difference is near-zero, but if a debris strike imparts an unmodeled torque a difference will persist until the window moves past the debris strike. This would produce a sustained change in \mathbf{H}^* for detection via the CUSUM SPRT.

4 RESULTS FROM ALGORITHMS

The CUSUM SPRT algorithm is run on clean angular momentum telemetry for each spacecraft to produce MMOD strike detection results. However, **these results have not yet been validated via comparison to MMOD flux models and other strike detection methods.** Section 5 discusses intended validation efforts and potential causes of false alarms.

4.1 SDO Results

The CUSUM algorithm applied to SDO's telemetry indicates frequent small MMOD impacts and occasional larger MMOD impacts. Figure 5 shows the summarized results for 2016. Figure 5(a) shows the number of strikes each day, while 5(b) shows the magnitude of the largest strike each day. These results exclude anything detected in the vicinity of mission events that cause an apparent change in body-frame angular momentum. Roughly 10 small strikes are detected most days but there are periods of higher activity and lower throughout the year. These periods of higher activity do not correlate to known micrometeoroid streams and their source has not been identified, but similar peaks are found in 2018 data. Figure 7 shows an example of typical small strike detections. Figure 6 shows the raw telemetry from

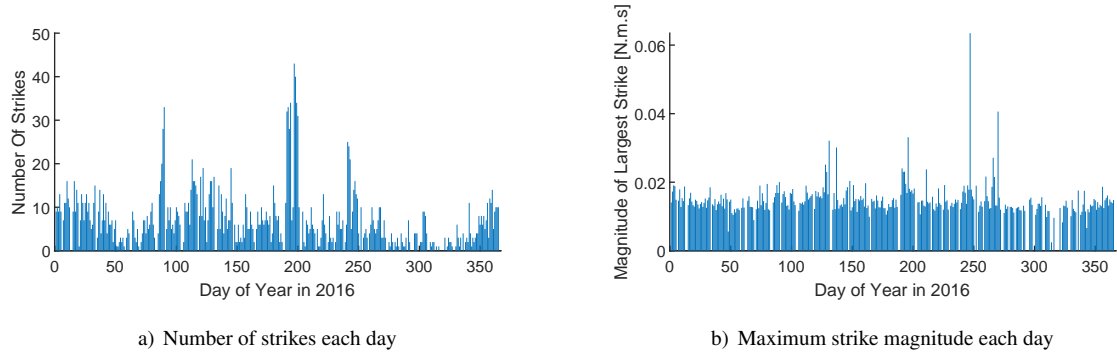


Figure 5: Results from SDO telemetry in 2016

the two largest events, on day 247 and 270. The event on day 247 exhibits an abrupt momentum change (Figure 6(a)) but then an unexpected oscillation. The reaction wheel telemetry (Figure 6(b)) shows odd data preceding the time of the event. Based on this, this event is not perceived to be a strike but is some other phenomenon. Its cause has not been identified. The second strike, on day 270, exhibits telemetry that is more aligned with expectations. The angular momentum changes abruptly (Figure 6(c)), and the spacecraft exhibits an increase in angular rate (Figure 6(d)) but it is corrected by the attitude control system.

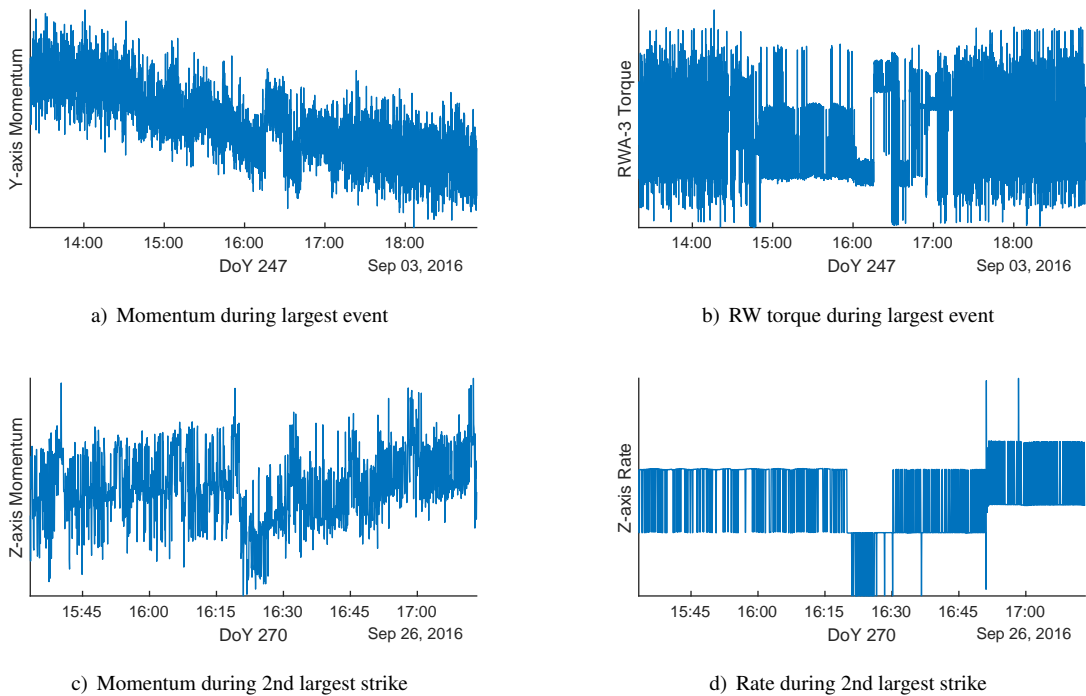


Figure 6: Results from SDO telemetry in 2016

It is important to note that these detections are not validated against other methods, they are just the data returned by this specific algorithm. In the case of SDO, the filtering required to clean the telemetry has been known to produce false detections at the junction between two sets of filtered data. This is rectified in this telemetry by filtering 10 days at a time and blanking the data at the intersection between filter sets, so filtering residuals are not known to cause false alarms in this telemetry. However, the potential for filtering to induce transients that manifest as MMOD strikes should not be ignored. Checkpointing provides some confidence that these detections are real momentum transfers by showing that the raw, unfiltered momentum data does exhibit step changes at the detected MMOD strikes. However, the estimated magnitudes are highly suspect. The magnitudes are estimated by differencing the average between the pre-window and the post-window. The noise floor of this estimate, even when no strikes are present, is significant, and the estimated sizes are only marginally higher than the noise. Therefore these estimates should not be taken as accurate until further modeling and validation is performed.

4.2 MMS Results

MMS is a difficult spacecraft to evaluate because of its long appendages and lack of 3-axis stabilization. The known debris strikes manifest as increased noise due to wire boom oscillation causing changes in the apparent inertial momentum. The noise in the inertial momentum also exceeds the noise in SDO's momentum significantly, sometimes by as much as an order of magnitude, making it more difficult to detect subtle changes.

The MMS-2 spacecraft and MMS-4 spacecraft are each evaluated. For MMS-4 300 days from 2016 are examined and for MMS-2 all of 2018 is evaluated. These years are selected because there is a known debris strike in each year which can be used to validate the debris detection algorithms. Due to the effects discussed in Section 2, significant portions of the MMS telemetry must be blanked to avoid false alarms. In these results 10 days are blanked after each thruster firing and all perigee passages are blanked. Figure 8 shows some example filter output, with a known debris strike observable but overwhelmed by the wire boom oscillations caused by thruster firing.

The MMS-4 spacecraft's results in 2016 are as follows. Figure 9(a) shows a plot of the results from all 300 days analyzed. The output of the CUSUM filter is plotted whenever any of the three axes are above the detection threshold. The grey bars are times when the output was blanked due to mission events, either perigee passages or thruster firings. The known debris strike in February causes a clear blip. However, it is overshadowed by large signatures resulting from perigee disturbances that exceed the blanked window, because in April through September the typical perigee disturbances shift so that they are outside the blanked window. To blank all of them would require substantially longer windows, resulting in the loss of large percentages of the data. An example of these extended perigee disturbances is shown in Figure 9(d).

A known debris strike is shown in Figure 9(c), where the debris strike shows a distinct signature. The signature persists for some time because the strike excites appendage oscillation causing the observed inertial momentum to oscillate. It takes a couple days for those oscillations to damp out. The raw momentum is shown in Figure 9(e).

There are also occasional significant features of unknown origin, one from April 6th is shown in Figure 9(c). In this feature the inertial momentum of the spacecraft increases for about an hour then decreases for about an hour, implying that a mild torque is applied to the spacecraft during this time period. This occurs while the spacecraft is near apogee, at an altitude of 76,000 km. The thruster firing telemetry does not indicate any firing events, and the origin of the torque has not been determined. Figure 9(f) shows the momentum telemetry during this event and also during a normal perigee passage. As shown, this event causes a slight dip and then return to typical values, while the perigee passage produces a more distinct feature and a net change in inertial momentum.

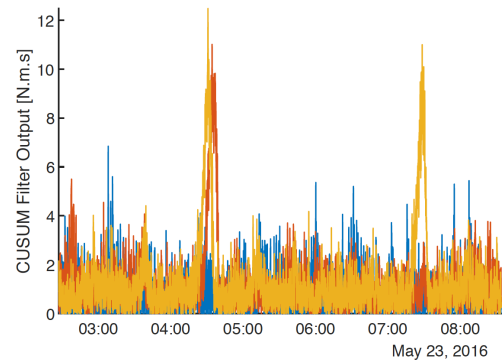


Figure 7: Example filter output from SDO showing two potential strikes

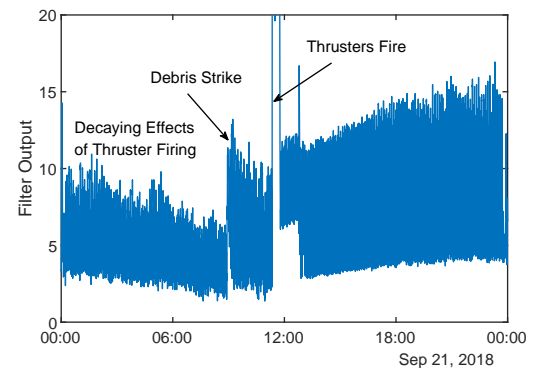


Figure 8: Example filter output from MMS-2

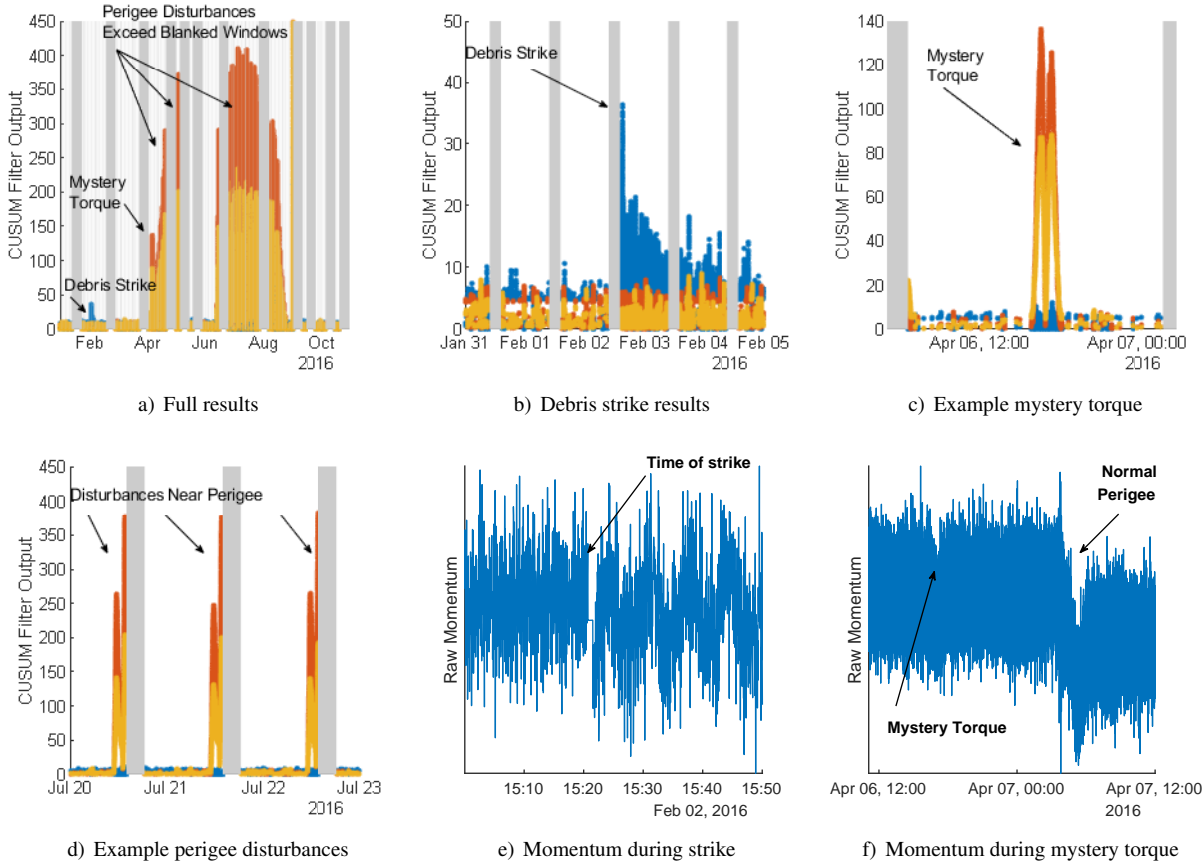


Figure 9: Results from MMS-4 telemetry in 2016

The MMS-2 results in 2018 are similar to the MMS-4 results but significantly cleaner, with only a few days of perigee effects that extend past the blanked window. The known debris strike occurs at a time when the telemetry was blanked due to a previous thruster firing, so it would have been missed without *a priori* knowledge of the strike. The telemetry is shown in Figure 8, which shows the filter output decaying over time as the oscillations from the previous thruster firing damp out, then an increase in oscillations from the debris strike, then a huge spike followed by decaying oscillations from another thruster firing. The summarized results are shown in in Figure 10. Comparing these to SDO's summarized results there are marginally fewer detections but still comparable, especially considering that SDO is in GEO, a highly used orbit likely to have significant populations of untracked debris, while MMS is in a highly elliptic orbit dissimilar from most other spacecraft.

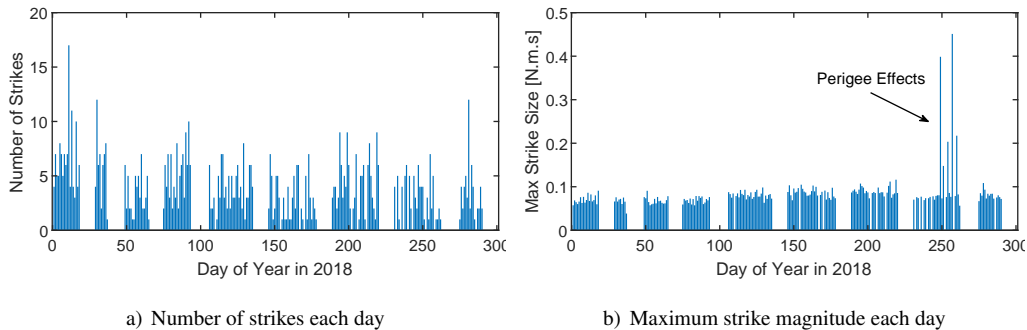


Figure 10: Results from MMS-2 telemetry in 2018

However, the discrepancies between the measured strikes' sizes are significant and imply that the measurements are not accurate. As mentioned in the SDO results, the measured size of the detected strikes (ΔH) is only marginally above the noise floor. This is also the case for the MMS ΔH measurements, but the MMS noise floor is a little higher and therefore the measurements are also a little higher. Further validation is required to determine the authenticity of these small strike detections. Validation methods are discussed further in Section 5.

The summarized MMS-4 results exhibit significantly higher strike counts, around 40 per day. However, they do not exhibit the clear spikes that SDO's results do, so it is expected that this 40/day is just noise. This implies that the noise levels are not consistent from spacecraft to spacecraft within the constellation, or perhaps from year to year. A refined method of adjusting the thresholds based on the dataset is in development to avoid these issues.

4.3 Fermi Results

The Fermi processing algorithm described in Section 2 represents a first-order solution, and the results indicate that more refinement is needed before the data can be used to detect debris strikes. Figure 11 shows the preliminary results. The inertial angular momentum is changing due to use of the torquer bars, but the proxy momentum, H^* , is relatively quiescent in comparison as desired. However, there are still significant features in H^* that manifest as debris strikes in the detection algorithms, so more refinement is needed before H^* can be used to detect debris strikes. A higher-order propagation for applying \dot{H} to determine H^* will be investigated, as well as smoothing to account for measurement errors. The spacecraft can also be simulated and the methods applied in simulation to validate the approach

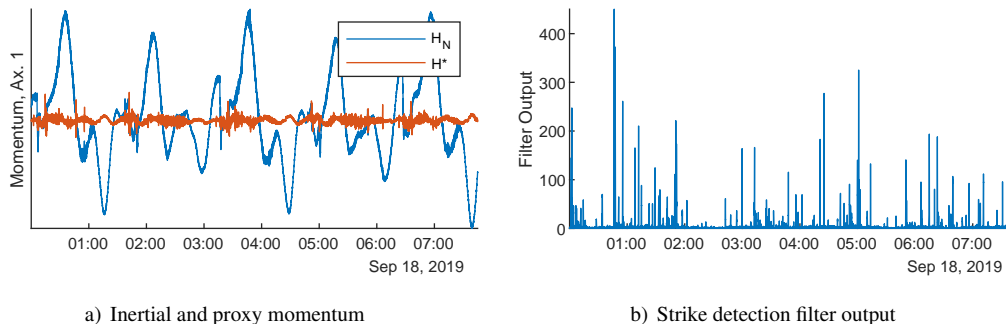


Figure 11: Preliminary results from Fermi telemetry

5 DISCUSSION AND FUTURE WORK

The results from the large strike events on SDO and MMS indicate that these methods have potential for accurately detecting unexpected momentum transfers indicative of debris strikes. However, the results for the small impacts are tenuous and will require validation from other sources to ensure that they are real impacts and not noise. Potential validation methods include cross-checking detections with other strike detection methods, such as strikes on antennas which have been measured on MMS and other spacecraft per [9], which generally occur several times per day depending on the detector. Models for expected micrometeoroid impacts, both flux and magnitude, will be developed for each spacecraft analyzed. If the momentum transfer detection results correspond to known micrometeoroid fluxes that would provide strong evidence that the detections are accurate. Currently the detected magnitudes are higher than would be expected from dust impacts. Additional spacecraft can be assessed to see if they generate similar results, particularly relatively quiescent 3-axis stabilized spacecraft like SDO, and spacecraft with highly accurate attitude control and thus improved ability to detect perturbations. The micrometeoroid flux should be fairly consistent between various orbits but the debris flux can show substantial variation. Impact detection results that align with these expectations would increase confidence in accurate detections.

One of the key challenges of analyzing on-orbit data is coping with unexpected disturbances which can manifest as debris strikes. MMS in particular shows substantial reactions to unexpected torques which obfuscate the debris strike signatures. These were originally thought to be gravity gradient torques since they usually occur at perigee, but some torques occur at slightly different times relative to perigee, and occasionally occur at much higher altitudes. The leading theory now is that they are caused by interaction between the charged spacecraft with long appendages and Earth's changing electromagnetic field. Another potential cause of unexpected angular momentum disturbances is electrostatic discharge (ESD), reference [10] discusses ground tests measuring impulses produced by ESD events.

A primary objective of this analysis is providing data for validating models of hazardous untrackable debris. Per the NESC report [7], current LEO models seem overly conservative and the cause has not been conclusively identified. However, based on seven observed impact events a major contributor could be the assumption that the debris can be modeled by an aluminum sphere with equivalent characteristic length. Alternate, less massive shape assumptions lead to better correlation between models and data. The methods applied in this paper offer the ability to measure the impact momentum directly. This can augment radar measurements of debris population sizes with more realistic mass estimates, which is critical since damage correlates to momentum better than to characteristic length. One challenge of measuring this momentum transfer is accurate characterization of the momentum enhancement factor (MEF), since the measured momentum could differ from the debris' relative momentum by a factor of 2 or more. Ongoing efforts to characterize MEF such as [11] must be incorporated as this research progresses to produce accurate data.

6 CONCLUSIONS

While challenges abound when applying these methods to on-orbit telemetry, the overall results are promising. The filters respond accurately to known debris strikes and detected several instances of unexpected momentum transfers on SDO, many of which are likely debris strikes. While detection and estimation near the noise floor is difficult and uncertain, the larger detections are more relevant. The debris that could potentially damage a spacecraft would necessarily have larger relative momentum and be more easily detectable. Therefore, these methods can be used to detect benign debris strikes that might otherwise be missed, and the results can be leveraged to improve models and risk assessments, monitor satellite state of health, and serve as a tool in anomaly attribution.

ACKNOWLEDGEMENTS

This work was supported by a NASA Space Technology Research Fellowship, NASA grant 80NSSC18K1142.

REFERENCES

- [1] “Monthly Number of Objects in Earth Orbit by Object Type”. In: *Orbital Debris Quarterly News* Volume 23.1 (May 2019).
- [2] Stephen Clark. “Investigators conclude external forces killed an Intelsat satellite in April”. In: *Spaceflight Now* (July 30, 2019).
- [3] H. Krag et al. “A 1 cm space debris impact onto the Sentinel-1A solar array”. In: *Acta Astronautica* 137 (Aug. 2017), pp. 434–443.
- [4] Trevor Williams, Joseph Sedlak, and Seth Shulman. “Magnetospheric Multiscale Mission Micrometeoroid/Orbital Debris Impacts”. In: *Spacecraft Anomalies and Failures Workshop 2017*. Chantilly, VA, Dec. 12, 2017.
- [5] G.A. Graham et al. “The chemistry of micrometeoroid and space debris remnants captured on hubble space telescope solar cells”. In: *International Journal of Impact Engineering* 26.1 (Dec. 2001), pp. 263–274.
- [6] Michael Squire. “Micrometeoroid and Orbital Debris Testing on Composite Overwrapped Pressure Vessels”. 2019 Applied Space Environments Conference. Los Angeles, CA, May 15, 2019.
- [7] *Evaluation of Micrometeoroid and Orbital Debris (MMOD) Risk Predictions with Available On-orbit Assets*. NASA Engineering and Safety Center Technical Assessment Report NESC-RP- 14-01000. NASA Engineering and Safety Center, Oct. 13, 2017.
- [8] Anne Aryadne Bennett, Hanspeter Schaub, and Russell Carpenter. “Assessing Debris Strikes in Spacecraft Telemetry: Development and Comparison of Various Techniques”. In: *70th International Astronautical Congress*. Washington, D. C., Oct. 21–25, 2019.
- [9] Ingrid Mann et al. “Dust observations with antenna measurements and its prospects for observations with Parker Solar Probe and Solar Orbiter”. In: *Annales Geophysicae Discussions* (July 15, 2019), pp. 1–39.
- [10] Alexander L. Bogorad et al. “Electrostatic Discharge Induced Momentum Impulse From Charged Spacecraft Surfaces”. In: *IEEE Transactions on Nuclear Science* 53.6 (Dec. 2006), pp. 3607–3609.
- [11] Robin Putzar et al. “How Hypervelocity Impacts Can Affect the LISA Mission – The MIRAD Study”. In: *International Astronautical Congress*. Washington, D. C., October 21 - 25, 2019.